Institute of Occupational Safety and Health Journal 9:225-239 (2001)

Capture Envelope of a Hood Opening under Crosswind Condition- A Numerical Approach

Yu-Kang Chen[1] , Rong-Fung Huang[2] , Chung-Wan Chen[3]

[1] Department of Occupational Safety and Hygiene, Chang Jung Christian University Kway Jen

[2] Department of Mechanical Engineering, National Taiwan University of Science and Technology

[3] Institute of Occupational Safety and Health, Council of Labor Affairs, Executive Yuan

Abstract

The flow induced by an exhaust opening will form a capture envelope in the presence of a crosswind. All streamlines located within the envelope will lead to the opening; those outside the envelope will lead to infinite downstream. The capture performance of the opening under crosswind then is determined by the extent of the capture envelope.

In this study, the opening on an infinite wall served as a model of an exterior hood used in a local exhaust device. The flow field was computed by potential flow theory by superposing the exhaust airflow on the uniform crosswind. The boundary of the capture envelope then was determined from the limiting streamlines found by iterative computation. The geometrical parameters of the envelope normalized to the diameter of the opening were found to be a function of the ratio of exhausted face velocity at the opening to the crosswind velocity, V_f / V_c. Based on the results obtained by extensive computations, and a pattern modified from the classical "Rankine's nose" problem, the empirical geometry of the envelope was obtained. The result was consistent with the case of "Rankine's nose" at $V_f / V_c \to \infty$; while $V_f / V_c < 2$, the pattern was further modified to fit the computed results.

Accpted 15 March 2001

* Correspondence to: Yu-Kang Chen, Department of Occupational Safety and Hygiene, Chang Jung Christian University, 396, Chang-Jung Rd. Sec.1, Kway-Jen, Tainan, Taiwan, 711, ROC. E-mail: ykchen@mail.cju.edu.tw

Keywords: Potential flow, Hood, Rankine's nose, Capture envelope

Introduction

The presence of a crosswind will affect the performance of an exterior hood dramatically[1-2]. Based on the knowledge from a classical "Rankine's nose" or "semi-infinite body" problem, in which the opening shrinks to a sink the exhaust airflow combining the crosswind forms a capture envelope in front of the hood[3-5]. All streamlines within the envelope lead to the hood opening, those outside of the envelope lead to infinity. Therefore, contaminant released inside the envelope tends to be captured by the hood; otherwise, it tends to escape the hood.

Theoretically, the flow field must be available in order to evaluate the capture performance of an exhaust opening in the presence of a crosswind. Earlier theoretical studies of hood performance mainly concerned the airflow velocity generated by the hood[2, 6-9]. The researches on the capture performance are relatively limited.

In this study, the hood was modelled by a circular opening on an infinite wall. The capture envelopes formed by the combination of the exhaust airflow and a uniform crosswind was computed numerically based on the potential flow theory. The general geometric pattern of the envelope then was determined by compiling the results from extensive computations. By employing potential theory, a finite exhausting opening in a crosswind is essentially an extension of the Rankine's nose problem. The potential theory is the simplest method to calculate the flow field generated by this system. Several studies have confirmed that the potential flow theory gives a plausible flow field induced by an exhaust opening, as compared with the results obtained by experiments or more sophisticated computations[1,6-7,9]. A recent study conducted in a wind tunnel also justified the existence of capture envelopes and their consistency with computation based on the potential flow theory[10].

Coordinate System and Flow Field

The center of a circular opening with a diameter D is located at the origin. The opening lies on an infinite wall defined by z = 0. A uniform crosswind with velocity V_c is in the x-direction. Hence, the z-axis is the central axis of the opening. The airflow is exhausted through the opening with a flow rate Q (Fig.1). The normal component of the exhaust flow is uniform on the opening face. Therefore, the normal airflow on the opening is $V_f = 4Q/(\pi D^2)$. Both crosswind and exhaust are assumed to be potential flow. Only the flow field within $z \geq 0$, or in front of the opening, is considered. The infinite wall effectively reflects the flow field back into itself.

Therefore, the imaging technique can be employed, and the exhausting effect is doubled.

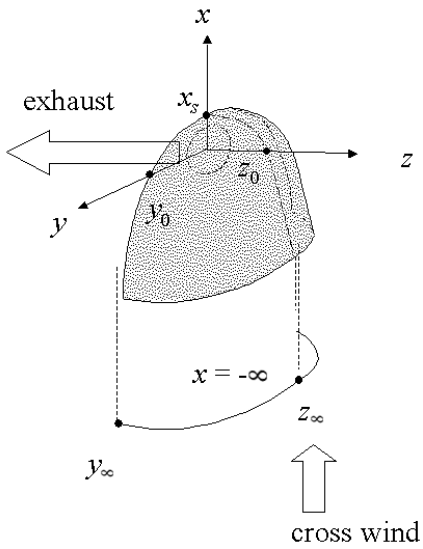

Figure 1 The coordinate system with a circular exhausting opening on an infinite wall in the presence of a cross wind and the geometry of a resulted capture envelope governed by x_s, y_0, z_0, y_∞ and z_∞.

The flow field was established by direct superposition of the uniform crosswind on the exhaust flow. With any given starting point (x, y, z) in front of the opening, the streamline, or the trajectory, can be computed numerically, by using Runge-Kutta 4-th order scheme[11], from

$$\frac{d\boldsymbol{x}}{dt} = \boldsymbol{V}_c + \boldsymbol{V}_o, \quad \cdots\cdots\cdots\cdots\cdots\cdots\cdots\cdots \quad (1)$$

where $\boldsymbol{x}$ is the space vector, and $\boldsymbol{V}_c$ and $\boldsymbol{V}_o$ are the velocity vector of the crosswind and the exhaust airflow, respectively. The capture envelope was revealed after sufficient starting points were used for streamline computation. A point is inside the envelope if a streamline starting from it leads to the opening; otherwise, it is outside the envelope. Therefore, with given Q, D, V_c, x and y, by judging the destination of the streamline starting from (x, y, z), the boundary of the envelope $z = f(x, y)$ can be found by iterative computation. The streamline on the boundary is a limiting streamline.

Geometry of a Capture Envelope

At $D \to 0$, the boundary of a capture envelope becomes a Rankine's nose with a infinite wall as its central plane, the geometry of the boundary is describe by[5]

$$\frac{x}{R_\infty} = \frac{1 - 2(r_x / R_\infty)^2}{2\sqrt{1 - (r_x / R_\infty)^2}}, \quad \cdots\cdots\cdots\cdots\cdots\cdots \quad (2)$$

in which, $r_x = \sqrt{y^2 + z^2}$ is the radial coordinate related to x-axis,

$$R_\infty = \sqrt{\frac{2Q}{\pi V_c}}, \quad \cdots\cdots\cdots\cdots\cdots\cdots\cdots\cdots \quad (3)$$

is the radius of the envelope normal to x-axis at $x \to -\infty$, or infinite upstream. The "2" in above equation is the effect of the imaging by the infinite wall. For a finite opening, R_∞ can be defined as

$$R_\infty = D\sqrt{\frac{V_f}{2V_c}} \quad , \quad \cdots\cdots\cdots\cdots\cdots\cdots\cdots\cdots \quad (4)$$

due to $Q = V_f \pi D^2 / 4$.

Define x_s and r_0 as the extent of the Rankine's nose in the direction of x and r_x measured from the origin, respectively. Since a Rankine's nose bears the geometry relation of $x_s = R_\infty / 2$ and $r_0 = R_\infty / \sqrt{2}$, Eq.(2) then can be rewritten as

$$\frac{x}{x_s} = \frac{1-(r_x / r_0)^2}{\sqrt{1-(r_x / R_\infty)^2}} \quad , \quad \cdots\cdots\cdots\cdots\cdots\cdots\cdots \quad (5)$$

For a finite opening, as modified from Eq.(5), the cross section of the envelope on the *xy*- and *xz*-plane ($z = 0$ and $y = 0$, respectively) normalized to D were assumed to be

$$\frac{x}{D} = \frac{x_s}{D}\frac{1-\left(\frac{y_c / D}{y_0 / D}\right)^2}{\sqrt{1-\left(\frac{y_c / D}{y_\infty / D}\right)^2}} \quad , \quad \cdots\cdots\cdots\cdots\cdots\cdots \quad (6)$$

and

$$\frac{x}{D} = \frac{x_s}{D}\frac{1-\left(\frac{z_c / D}{z_0 / D}\right)^2}{\sqrt{1-\left(\frac{z_c / D}{z_\infty / D}\right)^2}} \quad , \quad \cdots\cdots\cdots\cdots\cdots\cdots \quad (7)$$

respectively. In above equations, $y_c = y_c(x)$ is the cross section of the envelope on *xy*-plane, $z_c = z_c(x)$ is the cross section of the envelope on *xz*-plane, y_0 and z_0 are the extents of the envelope along the y- and z-axes, respectively, y_∞ and z_∞ are the extents of an envelope at $x \to -\infty$ in *y*- and *z*-directions, respectively. The cross section of an envelope normal to the x-axis, assumed to be a half-ellipse, is given by

$$\frac{z}{D} = \frac{z_c}{D}\sqrt{1-\left(\frac{y}{y_c}\right)^2} \quad , \quad \cdots\cdots\cdots\cdots\cdots\cdots \quad (8)$$

As seen in Eqs.(6) to (8) and Fig.1, the geometry of an envelope is controlled by five parameters: x_s, y_0, z_0, y_∞ and z_∞.

After normalized with D, these parameters were found to be a function of V_f / V_c only. Through extensive computations by varying V_f / V_c, the normalized parameters on the center-plane (*xz*-plane) was found to be fit by

$$\frac{x_s}{D} = \frac{1}{2}\sqrt{\frac{2.78/2}{\exp(2.78V_c / V_f)-1}+1} \quad , \quad \cdots\cdots\cdots \quad (9)$$

$$\frac{z_0}{D} = \frac{1}{2}\sqrt{\frac{1}{2}\left[-1+\sqrt{1+4\left(\frac{V_f}{V_c}\right)^2}\right]} \quad , \quad \cdots\cdots\cdots \quad (10)$$

and

$$\frac{z_\infty}{D} == \frac{4(V_f / V_c)^3 + 3V_f / V_c}{4\sqrt{2}(V_f / V_c)^{5/2} + 3(1+V_f / V_c)} \quad , \quad \cdots\cdots \quad (11)$$

Equation (9) is deduced from the stagnation point on the flange. The radial exhausted velocity related to the *z*-axis on the flange

was found empirically to be

$$\frac{V_{rz}(r_z)}{V_f} = \frac{1}{2.78}\ln\left[1+\frac{1}{2}\frac{2.78}{(2r_z/D)^2-1}\right],$$

in which, $r_z = \sqrt{x^2+y^2}$ is the radial coordinate related to z-axis. The stagnation point then can be found by $V_{rz}(x_s) = V_c$, which gives Eq.(9).

The extent of the envelope on z-axis was determined by computing the opening face velocity required to contain a given point on *z*-axis in the envelope. The required opening face velocity was fit by

$$\frac{V_f}{V_c} = 4\left(\frac{z_0}{D}\right)^2\sqrt{\left(\frac{D}{2z_0}\right)^2+1},$$

which gave Eq.(10).

The other parameters then were determined by the flow conservation and a half-elliptic cross section of the envelope normal to the crosswind. As shown in Fig. 2(a), the uniform crosswind enters the capture envelope at infinity upstream ($x \to -\infty$) is exhausted to the opening, this gives $Q = V_c \pi y_\infty z_\infty / 2 = V_f \pi D^2/4$, and

$$\frac{y_\infty}{D} = \frac{V_f/V_c}{2z_\infty/D} = \frac{4\sqrt{2}(V_f/V_c)^{5/2}+3(1+V_f/V_c)}{8(V_f/V_c)^2+6}, \quad \cdots\cdots (12)$$

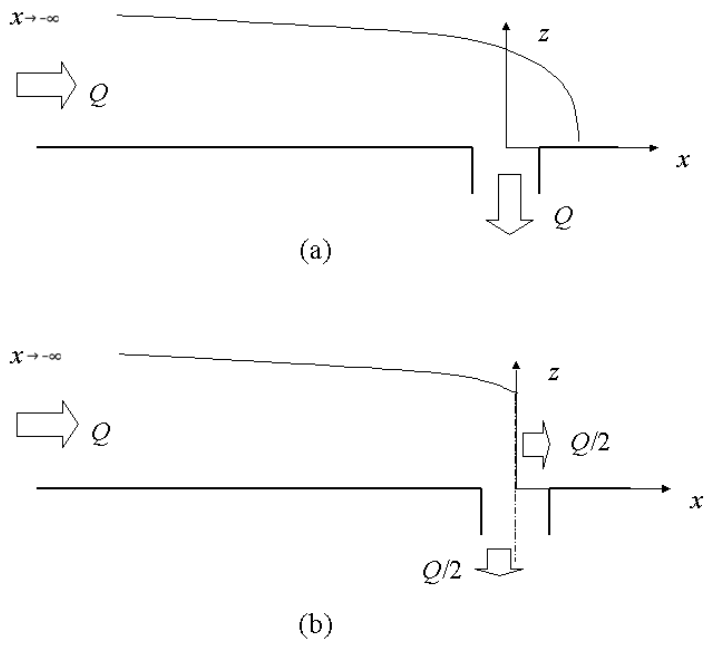

Figure 2 The flow conservation in the capture envelope.

Also, as shown in Fig. 2(b), at the cross section on the *yz*-plane (x = 0), half of the crosswind enters the opening, the other half enters the envelope downstream, this results in $Q/2 = V_c \pi y_0 z_0 / 2 = V_f \pi D^2 / 8$, and

$$\frac{y_0}{D} = \frac{1}{4}\frac{V_f/V_c}{z_0/D} = \frac{V_f/V_c}{\sqrt{2\left[-1+\sqrt{1+4\left(\frac{V_f}{V_c}\right)^2}\right]}}, \qquad (13)$$

Eqs.(9) to (13) are compared with the corresponding computations in Fig.3.

The computed results of y_∞ / D and z_∞ / D shown in Fig.3 were determined by extrapolation. The extent of the envelope in *y*- and *z*-directions are computed at an upstream far away from the opening, say $x/D = -5/2$, as y_{c5} and z_{c5}, respectively. From Eqs.(6) and (7), it gives

$$\frac{y, z_\infty}{D} = \frac{y, z_{c5}/D}{\sqrt{1-\left(\frac{2}{5}\right)^2\left(\frac{x_s}{D}\right)^2\left[\left(\frac{y, z_{c5}}{y_{c0}}\right)^2 - 1\right]}}, \quad \cdots (14)$$

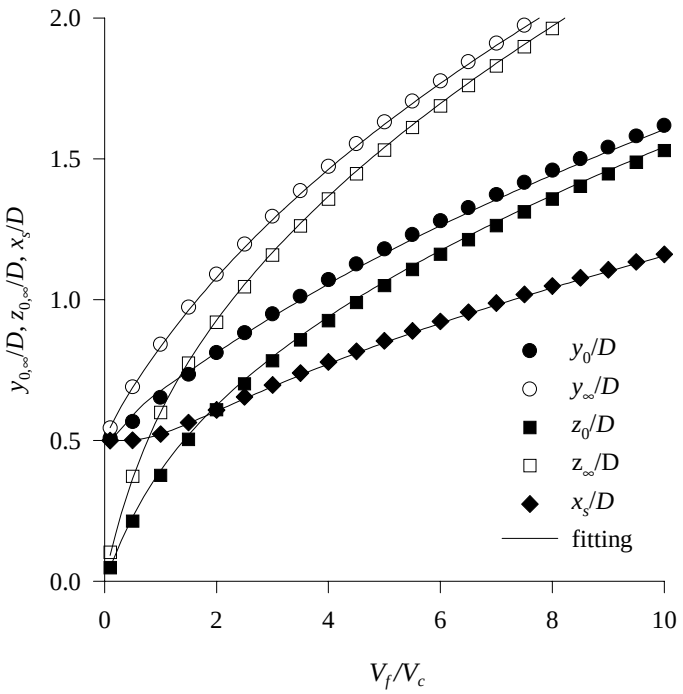

Figure 3 The computed results of y_0/D, y_∞/D, z_0/D, z_∞/D, and x_s/D in term of V_f/V_c and the corresponding fitting curves defined by Eqs.(9) to (13).

As $V_f / V_c \to \infty$, Eqs.(9) to (13) give $x_s / D \to \sqrt{V_f / (2V_c)} / 2$, y_0 / D and $z_0 / D \to \sqrt{V_f / V_c} / 2$, y_∞ / D and $z_\infty / D \to \sqrt{V_f / 2V_c}$, the extents exactly define a Rankine nose imaged by an infinite wall. While $V_f / V_c > 7$, the differences of all the extents to the corresponding limiting values will generally be smaller than 5%, from Eqs.(2) and (4), the boundary of the envelope may be approximated by

$$\frac{V_f}{V_c} = \frac{4\sqrt{(x/D)^2 + (y/D)^2 + (z/D)^2} \times}{\left[x/D + \sqrt{(x/D)^2 + (y/D)^2 + (z/D)^2}\right]}, \quad \cdots\cdots\cdots\cdots\cdots\cdots\cdots\cdots\cdots\cdots \quad (15)$$

As observed in the experiments conducted in a wind tunnel. The empirical extents of the capture envelope on the central plane were found to be[10]

$$\frac{x_s}{D} = 0.43\left(\frac{V_f}{V_c}\right)^{0.41}, \quad \cdots\cdots\cdots\cdots\cdots\cdots \quad (16)$$

$$\frac{z_0}{D} = 0.41\left(\frac{V_f}{V_c}\right)^{0.55}, \cdots\cdots\cdots\cdots\cdots\cdots \quad (17)$$

and

$$\frac{z_\infty}{D} = 0.62\left(\frac{V_f}{V_c}\right)^{0.49}, \quad \cdots\cdots\cdots\cdots\cdots\cdots \quad (18)$$

respectively. Figure 4 shows the comparison between above parameters and those fitted from the computation, as described by Eqs.(9) to (11). The comparison reveals a significant over-estimation on z_∞ / D by computation. However, an extent of a capture envelope at the infinite upstream of the crosswind is very difficult to be determined accurately in a real flow. The finite flange used in the experiments may account for the deviation. Figure 4 also shows a slight over-estimation of z_0 / D by computation, the computational result is still acceptable for the purpose of hood design. While $V_f / V_c = 0$, the computation gives $x_s / D = 0.5$ due to infinite exhaust velocity at the edge of the opening. The fitting from the experiments, which were conducted at $V_f / V_c > 3$, gave $x_s / D = 0$. The difference between both fittings of x_s / D becomes significantly at $V_f / V_c < 2$, which is too low for a common hood operation.

Figure 5 shows the cross sections of the envelope determined by both computation and approximation described by Eqs.(6) to (8). The approximated cross sections are generally consistent with those determined by computation. However, at lower V_f / V_c, as the cross sections become flatter, the approximation fails to describe the cross section accurately, particularly in the *z*-direction. However, the figure does justify that the envelopes have a half-elliptic cross section normal to *x*-axis.

At Small V_f / V_c

For smaller V_f / V_c, the results obtained

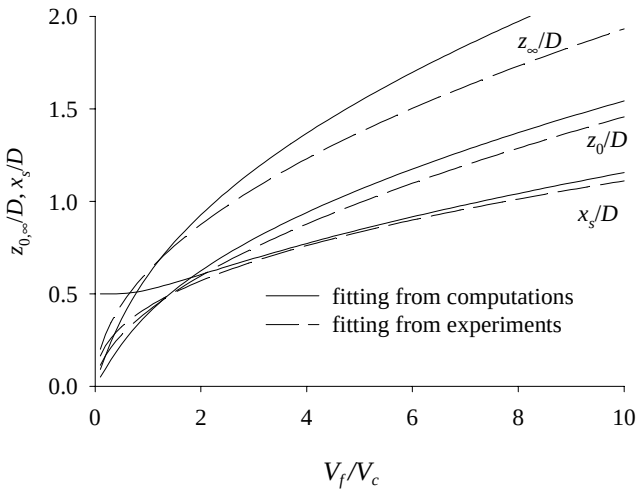

Figure 4 Extents of the capture envelope at the central plane. The solid lines indicate the fitting from the computation in this study (Eqs.(9), (10) and (11)); the dashed lines indicate the empirical relation determined from the experiment (Eqs.(16)-(18))[10].

by potential theory may no longer be valid since the resulted envelope becomes too close to the flange and opening where viscosity and rotation along with boundary layer, turbulence, separation and vena contracta become too significant to be neglected. In the potential theory, singularity is formed at the edge of the opening, where the flow velocity becomes infinitely large, a phenomenon can never occur in the real flow. Therefore, while V_f/V_c is extremely small, the boundary of the capture envelope may cross the opening face, and part of the exhausted airflow may re-enter the flow field. However, for theoretical completeness, we still conduct following analysis at small V_f/V_c.

Figure 6 shows the cross section of the envelope normal to the *y*-axis on *xz*-plane at different V_f/V_c. The coordinate x and z are normalized to x_s and z_∞, respectively. While $V_f/V_c > 2$, the pattern of the cross section does not vary significantly, and can be approximated by Eq.(7) properly. As V_f/V_c becomes smaller, the xz cross section is asymptotic to a pattern described by

$$\begin{cases} x = -2\dfrac{x_s}{z_\infty} z_c + x_s & \text{for } z_c < z_\infty \\ x = -\infty & \text{for } z_c \geq z_\infty \end{cases} , \quad \cdots\cdots\cdots (19)$$

with $z_\infty = 2z_0$. Eq.(7) is no longer an appropriate approximation. From Eqs.(9) and (10), as $V_f/V_c \to 0$, $x_s/D \to 1/2$ and $z_0/D \to V_f/(2V_c)$, the slope of the envelope boundary on xz-plane (measured from z-axis)

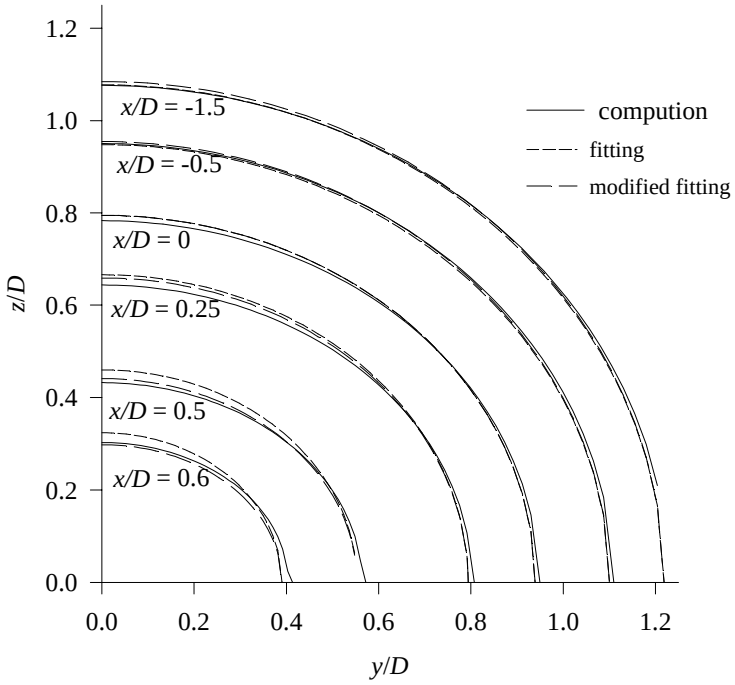

(a)

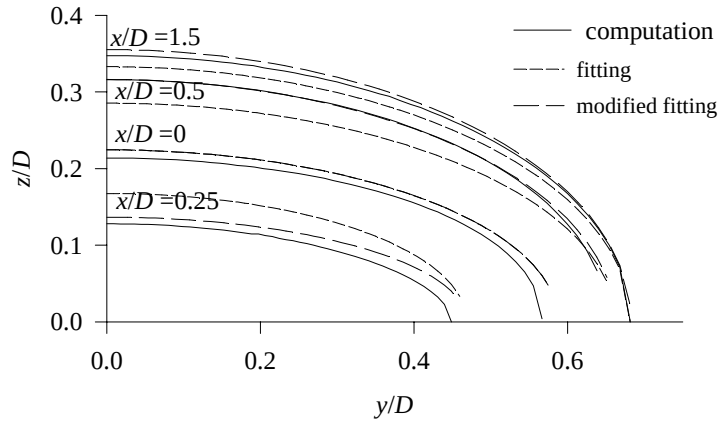

(b)

Figure 5 Cross sections of the capture envelope normal to x-axis at (a) $V_f / V_c = 3$; (b) $V_f / V_c = 0.5$. The solid lines are computed results; the short-dashed lines are approximated results using Eqs.(6) to (8); the long-dashed lines are modified fittings, as described by Eqs.(20).

then is $-x_s / z_0 \to -V_f / V_c$. This is due to a uniform exhaust velocity close to V_f in the proximity of the opening. Also, as $V_f / V_c \to 0$, $x_s / D \to 1/2$, $y_0 / D \to 1/2$ and $z_\infty / D \to V_f / V_c = z_0 / D$. Therefore, the straight line defined in Eq.(19) starts from the stagnation point on the wall (near the downstream end of the opening), and ends at a point perpendicular to the upstream end of the opening.

In order to perform a smooth transition from Eq. (7) to Eq.(19), a modified equation was introduced to describe the cross section of the envelope on *xz*-plane:

$$x = x_s \frac{1-(z_c / z_0)^\alpha}{\left[1-(z_c / z_\infty)^2\right]^\beta} , \quad \cdots\cdots\cdots\cdots\cdots \quad (20)$$

in which α and β are two parameters the shape of the cross section depends on. It requires that $\alpha \to 1$ and $\beta \to 0$ at $V_f / V_c \to 0$ to be consistent with Eq. (19); and $\alpha \to 2$ and $\beta \to 1/2$ at $V_f / V_c \to \infty$ to be consistent with a Rankine's nose described by Eq.(7).

Based on the computation on the cross section on the *xz*-plane, it was found that

$$\begin{cases} \beta = V_f / V_c & \text{for } V_f / V_c < 0.5, \\ \beta = 0.5 & \text{otherwise.} \end{cases} \quad \cdots\cdots \quad (21)$$

and

$$\alpha = \frac{z_0 / x_s}{V_f / V_c} \frac{\left[1-(z_0 / z_\infty)^2\right]^\beta}{1-\dfrac{2z_0 / D}{\sqrt{1+4(z_0 / D)^2}}} , \quad \cdots\cdots \quad (22)$$

Equation (22) makes the contour defined by Eq.(20) satisfy $dx / dz_c = V_c / V(0,0,z_0)$ at $z_c = z_0$, where $V(x,y,z)$ is the exhaust velocity at a given point (x, y, z). Along the *z*-axis, from potential flow theory, the analytical solution of the exhaust velocity is[9]

$$V(0,0,z_0) = -V_f \left(1 - \frac{z_0}{\sqrt{1+4(z_0 / D)^2}}\right), \quad \cdots\cdots (23)$$

The fittings of the cross section on the *xz*-plane were compared with the computational results in Fig.7. Figure 5 also shows the further modification improves the fitting dramatically at low V_f / V_c.

To complete the evaluation of the fitting, Fig. 8 shows the cross section of the envelope on xy-plane. The fitting based on Eq.(6) generally match the computed results, though the fitting cross section crosses the opening slightly (about 3% in radial direction) at $V_f / V_c = 0.1$. Figure 5(b) also reveals in a small fitting error on the cross section normal to x-axis at $V_f / V_c = 0.5$. Notably, as $V_f / V_c \to 0$, the cross section on xy-plane defined by Eq.(6) approaches

$$\frac{x}{D} = \frac{x_s}{D}\sqrt{1-(y_c / y_0)^2} , \quad \cdots\cdots\cdots\cdots\cdots\cdots (24)$$

it is a half-circle surrounding the opening at the downstream side.

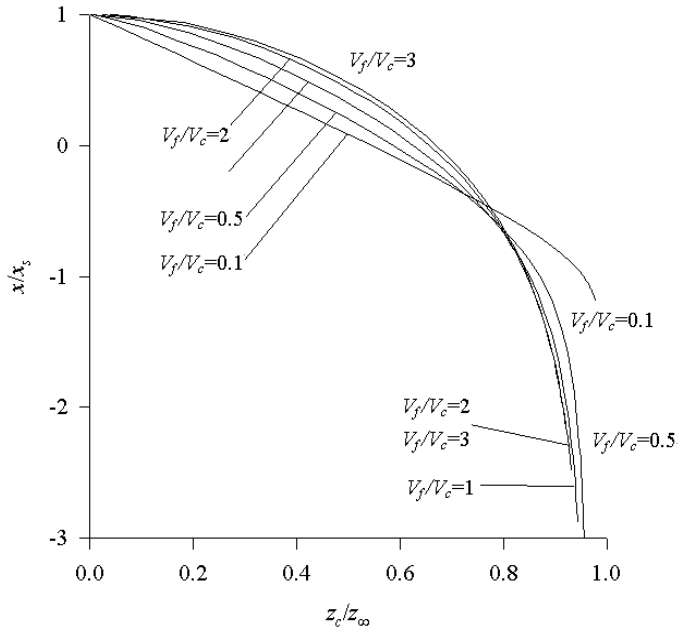

Figure 6 Cross sections of the capture envelope on *xz*-plane at different V_f / V_c.

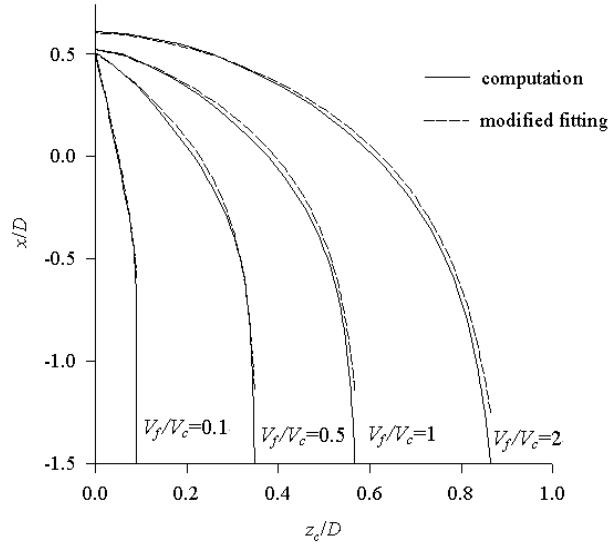

Figure 7 Cross sections of the capture envelope on xz-plane at different V_f / V_c. The computational results are shown by the solid lines; the modified fittings, as described by Eqs.(20) to (21), are shown by the dashed lines.

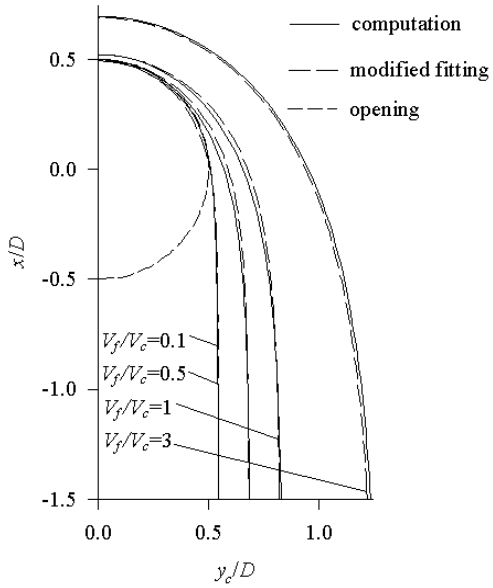

Figure 8 The cross section of the capture envelope on xy-plane, the solid lines are computed results, the long-dashed lines are fitting results (Eq.(6)), and the short-dashed lines are the edge of the opening.

Required Flow Rate to Capture Pollutant from a Point Source

Practically, it is necessary to evaluate the required flow rate to contain a given point (x, y, z) inside a capture envelope. To achieve this goal by employing fitting developed previously, a procedure is proposed as follows:

1. Give an initial V_f/V_c from given (x/D, y/D, z/D) by using Eq.(15). It gives a required facing velocity at opening relative to the crosswind to contain the given point inside the envelope.
2. Calculate x_s/D, y_∞/D, z_∞/D, y_0/D, z_0/D, α, and β from available V_f/V_c by using Eqs.(9), (12), (11), (13), (10), (22) and (21), respectively.
3. Calculate y_c/D by solving Eq.(6), it gives

$$\begin{cases} y_c/D = \frac{1}{4}\left\{-\beta_y + \sqrt{\beta_y^2 - 64(y_0/D)^4\left[1-(x/x_s)^2\right]}\right\} & \text{for } x<0, \\ y_c/D = \frac{1}{4}\left\{-\beta_y - \sqrt{\beta_y^2 - 64(y_0/D)^4\left[1-(x/x_s)^2\right]}\right\} & \text{for } x\geq 0. \end{cases} \quad \cdots\cdots (25)$$

in which

$$\beta_y = 4\left(\frac{y_0}{D}\right)^2\left(\frac{y_0 x}{y_\infty x_s} - 2\right), \quad \cdots\cdots (26)$$

4.Determine z_c/D from Eq.(8) as

$$\frac{z_c}{D} = \frac{z/D}{\sqrt{1-\left(\frac{y}{y_c}\right)^2}}, \quad \cdots\cdots\cdots\cdots \quad (27)$$

5. Determine the other x/D from Eq.(20) by considering the case of $z_c/D \geq z_\infty/D$ as

$$\begin{cases} \frac{x_1}{D} = \frac{x_s}{D}\frac{1-(z_c/z_0)^\alpha}{\left[1-(z_c/z_\infty)^2\right]^\beta} & \text{for} \quad z_c < z_\infty, \\ \frac{x_1}{D} = -\frac{1}{2}\{X + (z_c - z_\infty)\} & \text{for} \quad z_c \geq z_\infty, \end{cases} \quad (28)$$

in which X is a large value, say 100.

6. Vary V_f/V_c until $x/D - x_1/D$ converge to an acceptable tolerance. The Newton-Raphson scheme can be used for this purpose.

Then V_f/V_c calculated in Step 1 is served as an initial guess value. The second row in Eq.(28) is to provide a slope for convergence. Nowadays, this iteration can be performed in a commercial spreadsheet package, such as Microsoft™ Excel®, by invoking Solver function.

Conclusions

The capture envelope formed by the airflow induced by an exhaust opening combined with a uniform crosswind was computed based on the potential theory. The geometry of the capture envelope normalized to the diameter of the opening was found to be a function of V_f/V_c, the ratio of the face velocity at opening to the uniform crosswind velocity. While $V_f/V_c > 2$, the geometry of the envelope can de described by the pattern modified from Rankine's nose. For even larger V_f/V_c greater than 7, the geometry of the envelope was found to be similar to the Rankine's nose.

At smaller V_f/V_c, the geometric pattern modified from the Rankine's nose fails to describe the envelope. A further modification was made to result in a good fitting.

Acknowledgement

The authors wish to thank the Institute of Occupational Safety and Health, Council of Labor Affairs (Taiwan), Grant IOSH89-H104, for financial support.

References

[1] Flynn, M.R., Ellenbecker, M., 1986; "Capture Efficiency of Flanged Circular Local Exhaust Hoods" Ann. Occup. Hyg., 30:497-513.

[2] Flynn, M.R. and Ellenbecker, M., 1987; "Empirical Validation of Theoretical Velocity Fields into Flanged Circular Hoods" Am. Ind. Hyg. Assoc. J., 48:380-389.

[3] Batchelor, G.K., 1967; "An Introduction to Fluid Dynamics" Cambridge University

Press, London.

[4] Panton, R.L., 1984; "Incompressible Flow" John Wiley & Sons, New York.

[5] Yuan, S. W., 1967; "Foundation of Fluid Mechanics" Prentice-Hall, Englewood Cliffs, NJ.

[6] Flynn, M.R. and Ellenbecker, M., 1985; "The Potential Flow Solution for Airflow into a Flanged Circular Hood" Am. Ind. Hyg. Assoc. J., 46:318-322.

[7] Flynn, M.R., and Miller, C.T. 1988; "Comparison of Models for Flow through Flanged and Plain Circular Hoods" Ann. Occup. Hyg., 32:373-384.

[8] Conroy, L.M., Ellenbecker, M.J., and Flynn, M.R. 1988; "Prediction and Measurement of Velocity into Flanged Slot Hoods" Am. Ind. Hyg. Assoc. J., 49:226-234.

[9] Kulmala, I. 1993; "Numerical Calculation of AirFlow Fields Generated by Exhausted Openings" Ann. Occup. Hyg., 37:451-467.

[10] Huang, R. F., Chen, J. L., Chen, Y. K., Chen, C. C., Yeh, W. Y., Chen, C. W., 2001; “The capture envelope of a flanged circular hood in cross drafts” Am. Ind. Hyg. Assoc. J., 62:199-207.

[11] Press, H.P., Flannery, B.P., Teukolsky, S.A., and Vetterling, W.T., 1988; " Numerical Recipes in C: The Art of Scientific Computing" Cambridge, New York.

勞工安全衛生研究季刊　民國九十年九月　第九卷第三期　第 225-239 頁

抽氣開口在側風下所形成的捕集區—數值計算

陳友剛[1]　黃榮芳[2]　陳春萬[3]

[1]長榮管理學院職業安全與衛生系

[2]國立台灣科技大學機械系

[3]行政院勞委會勞工安全衛生研究所

摘　要

吸氣開口於側風中會在開口前方形成一捕集區，所有位於捕集區內的流線均會導入開口：所有位於捕集區外的流線則導入側風下游無限遠處。吸氣開口對氣流的捕集能力可由捕集區所涵蓋的範圍決定。

在本研究中，一位於無限平面上的圓形開口用以模擬計算外裝形氣罩的捕集能力。流場則採用勢流理論計算，將吸氣開口所產生的流場直接疊加於橫向均勻流場。捕集區的範圍則可利用分隔流線求得。經初步探討發現捕集區範圍參數對開口直徑的比值與側風對開口面平均風速比值，V_f / V_c，相關。將多次計算結果加以整理後，更發現捕集區的幾何形狀可根據 Rankine's 鈍體幾何形狀修正而得。當 $V_f / V_c \to \infty$ 上述結果與 Rankine's 鈍體幾何形狀完全相符。當 $V_f / V_c < 2$ 時，則需更進一步的修正，使捕集區經驗幾何形狀與計算結果更爲吻合。

關鍵詞：勢流、氣罩、Rankine's 鈍體、捕集區

民國 89 年 6 月 27 日收稿，89 年 10 月 6 日修訂，民國 90 年 3 月 15 日接受

通訊作者：陳友剛，長榮管理學院職業安全衛生系，台南縣歸仁鄉 711 長榮路一段 396 號，E-mail: ykchen@mail.cju.edu.tw